

Accepted Manuscript

Title: Organo functionalized graphene with Pd nanoparticles and its excellent catalytic activity for Suzuki coupling reaction

Author: Surjyakanta Rana Suresh Maddila Kotaiah Yalagala Sreekantha B. Jonnalagadda



PII: S0926-860X(15)30070-3
DOI: <http://dx.doi.org/doi:10.1016/j.apcata.2015.07.018>
Reference: APCATA 15467

To appear in: *Applied Catalysis A: General*

Received date: 6-5-2015
Revised date: 30-6-2015
Accepted date: 9-7-2015

Please cite this article as: Surjyakanta Rana, Suresh Maddila, Kotaiah Yalagala, Sreekantha B. Jonnalagadda, Organo functionalized graphene with Pd nanoparticles and its excellent catalytic activity for Suzuki coupling reaction, Applied Catalysis A, General <http://dx.doi.org/10.1016/j.apcata.2015.07.018>

This is a PDF file of an unedited manuscript that has been accepted for publication. As a service to our customers we are providing this early version of the manuscript. The manuscript will undergo copyediting, typesetting, and review of the resulting proof before it is published in its final form. Please note that during the production process errors may be discovered which could affect the content, and all legal disclaimers that apply to the journal pertain.

Organo functionalized graphene with Pd nanoparticles and its excellent catalytic activity for Suzuki coupling reaction

Surjyakanta Rana, Suresh Maddila, Kotaiah Yalagala and Sreekantha B. Jonnalagadda*

School of Chemistry & Physics and College of Agriculture, Engineering & Science, University of KwaZulu-Natal, Durban, South Africa

*Corresponding author: *Prof. Sreekantha B. Jonnalagadda School of Chemistry & Physics College of Agriculture, Engineering & Science, University of KwaZulu-Natal, Durban, South Africa*

Email: jonnalagaddas@ukzn.ac.za

Phone no: +27 31 260 7325/3090

Fax No-+27 31 260 3091

Graphical abstract

Highlights

- Pd(0) on AAPTMS@G an efficient catalyst for Suzuki coupling.
- Pd(0) AAPTMS@G gives 98% yield of biphenyl in 25 min.
- Remarkably stable and active up to six successive cycles.

Abstract

Synthesis of well distributed palladium nanoparticles (3 – 7 nm) on organo di-amine functionalized graphene is reported, which demonstrated excellent catalytic activity for Suzuki

coupling reaction. Organo functionalized graphene support acted as an excellent host which helped in avoiding “Ostwald ripening” i.e., preventing palladium nanoparticle sintering and because of which the catalyst as a whole showed excellent catalytic activity for Suzuki coupling reaction. The catalytic material was characterized by X-ray diffraction (XRD), Fourier-transfer infrared spectroscopy (FTIR), Raman spectra, X-ray photoelectron spectra (XPS), and Scanning electron microscope (SEM), Transmittance electron microscopy (TEM) analysis. FT-IR revealed that the organic amine functional group was successfully grafted onto the graphene oxide surface. The formation of palladium nanoparticles was confirmed by XPS techniques. The catalytic activity in the coupling reaction using iodobenzene was superb with 100% conversion and 98 % yield and also activity remained almost unaltered up to six cycles. Typically, an extremely high turnover frequency of 185,078 h⁻¹ or 3,084.64 min⁻¹ is observed in the C-C Suzuki coupling reaction using organo di-amine functionalized graphene as catalyst. Experiments were also conducted under identical conditions to prove heterogeneity of the catalyst.

Key words: Pd nanoparticle; Di-amine; Graphene oxide; Graphene; Suzuki coupling.

1. Introduction

Over a period of time, several carbon based supports such as graphite, activated carbon, carbon nanotubes (CNT) and graphene etc. have been developed to suit catalyst loading. In

past two decades, among the nanomaterials, CNTs have fascinated the researchers and industry, due to the amazing scientific and technological implications [1-4]. Wide range of applications including nano derivative fabrication, highly sensitive and rapid response with short reaction times are some of the attractions [5-7]. CNTs are considered to be promising nanomaterials for developing the next generation sensors, but their toxicity to living organisms is of concern [8]. Graphene which is nontoxic, two-dimensional material, having impressive properties, such as high surface area, high optical and electrical conductivity etc. is considered to be ideal as catalytic support [9-19]. Graphene oxide (GO) can be prepared from various sources and using different methods such as chemical vapor decomposition, (CVD) [20], arc discharge [21,22], Hummers [23], Hummers sonication [24] and wet chemical methods [25]. GO sheet contains various functional groups such as hydroxyl, epoxy and carboxylic groups. GO sheets can be chemically modified to have different substituents. The epoxy and carboxylic groups of GO sheet can be modified using appropriate organic moieties. The residual oxygen hanging group on chemically modified graphene oxide can serve as an attractive means for further attachment of the organic moieties. Graphene based complexes and GOs have potential applications in catalysis, sensor and energy fields. Currently researchers are focusing on the novel metal nanoparticles due to their mechanical, optical and chemical properties. These nanoparticles show high activity because of their sizes, shapes and rate of production when compared to the large particles and gaseous molecules.

Various metal modified supports like TiO_2 , ZrO_2 , SiO_2 , CeO_2 , Ce-Zr composites including graphene have been reported in the literature [26]. Organic and inorganic hybrid materials have added advantages to bind the metal strongly as compared to the normal support materials. The metal remains bound and does not leach, hence reusable for several cycles. Different metal modified amine functionalized supports like silica, clay have also been described in the literature [27]. Recently our group developed Pd(II) modified amine functionalized graphene

oxide for oxidation reaction [28]. Among the noble metals, palladium (Pd) found to be more attractive in the fields of nanotechnology and catalysis. However, size reduction of active metal particles results in a significant increase of the reactivity due to the high surface-to-volume ratio of small particles along with a large fraction of active atoms with dangling bonds exposed to the surface. Earlier reports described the important role of Pd nanoparticles as a catalyst in the synthesis of many organic and inorganic reactions [29]. Again, prevention of particle sintering is another important issue. Due to “Ostwald ripening” mechanism, bare particles without any supports or stabilizers are easily agglomerated, since larger nanoparticles are more energetically favored than smaller ones generating large clumps that decrease their initial activity during the reaction. Such agglomeration frequently happens under harsh reaction conditions. This work describes, the amine functionalized GO sheets stabilizing the Pd nanoparticles and also supplying adequate electron density to the anchored Pd(0) species to facilitate the oxidative addition of halobenzene to Pd(0). Additionally, carbon based nanoparticles show potential properties due to the synergistic effect of metal nanoparticle and carbon layer [30]. In organic reactions, Suzuki coupling reaction is one of the most powerful tools to prepare the bi-aryl structures that exist in the many biologically active complexes and natural products [18]. Consequently, Pd loaded functionalized graphene is ideal for a C-C coupling reaction.

Herein, we report for the synthesis of Pd nanoparticles (3 - 7 nm) deposited amine functionalized graphene. Furthermore, its exceptional scope as catalyst for C-C Suzuki coupling reactions in aqueous medium with excellent yields (98 %) is established. Experiments also showed that the catalyst is stable, reusable up to six cycles.

2. Materials and methods

2.1. Preparation of GO catalyst:

Initially, graphite powder (0.5 g) and NaNO_3 (0.5 g) were dissolved in concentrated H_2SO_4 (23 ml) with stirring for 20 min and the mixture was cooled on ice bath for 2 h. Then, the reaction mixture was put on hot plate with magnetic stirrer at 40 °C and KMnO_4 (6 g) crystalline powder was added slowly and stirring continued for 70 min. Then, distilled water (50 ml) was added to the mixture and stirred for further 20 min, followed by H_2O_2 (30 %) till the color of the solution changed from dark brown to yellow. Upon the colour change, water (50 ml) was added and the resulting solution was sonicated over 2 h. The solution was centrifuged, separated and filtered with double distilled water several times. The product was dried in a vacuum oven at 100 °C overnight to obtain GO.

2.2. Preparation of Pd (0)-AAPTMS@G catalyst:

GO (1 g) was dissolved in toluene (50 ml) in a conical flask and sonicated for 2 h. [3-(2-Aminoethylamino)propyl]trimethoxysilane (AAPTMS) (1.68 mmol) (Aldrich) was added to the above solution and sonicated for further 1 h. Next, powder palladium nitrate (0.46 mmol, 5 wt%) was added to the mixture and stirred for 4 h and 12 mmol of NaBH_4 was added and stirring was continued for further 1 h. The solution was centrifuged and the product was dried in a vacuum oven at 100 °C overnight to obtain Pd (0)-AAPTMS@G.

2.3. Physico-chemical analytical methods:

The powder X-ray diffraction (XRD) performed on a Bruker D8 Advance instrument, equipped with an Anton Paar XRK 900 reaction chamber, a TCU 750 temperature control unit and a $\text{CuK}\alpha$ radiation source with a wavelength of 1.5406 nm at 40 kV and 40 mA. Diffractograms were recorded over the range 15–90° with a step size of 0.5 per second. The TEM images were viewed on a Jeol JEM-1010 electron microscope. The images were captured and analysed by using iTEM software. High resolution TEM images were recorded by using Jeol JEM 2100 Electron Microscope. The SEM measurements were carried out using a JEOL

JSM-6100 microscope equipped with an energy-dispersive X-ray analyzer (EDX). Infrared spectra of the samples were recorded using Fourier transmission infrared (FTIR) spectrometer (PerkinElmer spectrum 100 series with universal ATR accessory). Raman spectra are collected on a Perkin Elmer 1200 Fourier Transform Infrared and on a DeltaNu advantage 532TM Raman Spectrometer (100 mW Nd: YAG laser with an excitation wavelength of 532 nm). The electronic structure aspects of the samples were investigated using KRATOS apparatus with Mg, Al, and Cu K α as X-ray sources by XPS.

2.4. General procedure for Catalytic reaction:

Iodobenzene (1 mmol) was added to the stirring mixture of tripotassium phosphate (0.0018 mmol), phenyl boronic acid (1.2 mmol), and deionized water (20 ml) followed by the addition of Pd(0)-diamine functionalized graphene(0.05g). The reaction mixture was then stirred at 90 °C for 25 min and extracted with ethyl acetate (Scheme 1). The organic layer was dried with anhydrous sodium sulfate (Na₂SO₄) and the resulting mixture was analyzed by gas chromatography (GC). The catalyst was recovered by the simple centrifugation and washed extensively with deionized water.

3. Results and Discussion:

The X-ray diffraction spectra of GO and Pd(0)-AAPTMS@G are illustrated in Figure 1. The pattern at $2\theta \approx 10.75$ is the characteristic diffraction peak (002) of GO [31, 32] and the other peak at $2\theta \approx 42.94$ corresponds to the plane of the carbon hexagonal structure (100) [31, 33]. After modification of both organo group and Pd of the GO sheets, the plane shifted (002) towards the higher angle at $2\theta \approx 23.11$, i.e. formation of graphene nano sheets due to the both sonication [34] and addition of metal borohydride to GO. The peaks appearing at $2\theta \approx 40.11$, 46.27 and 68.32 were due to the presence of Pd planes (111), (200), (220). This suggests the organo group and Pd incorporation onto the GO sheets.

The FT-IR spectra of GO, AAPTMS@GO and Pd(0)-AAPTMS@G samples are shown in Figure 2A (a-c). From this spectra(a), both 3400 cm^{-1} , 1740 cm^{-1} and 1385 cm^{-1} peaks were due to O-H stretching, C=O stretching of -COOH and O-H vibration of C-OH groups respectively and 1100 cm^{-1} was due to the epoxy group vibration. The spectra (b & c) show that peaks for carboxyl groups vanish [35] and only spectra showing N-H stretching at 3371 cm^{-1} and NH_2 bending mode of free NH_2 groups at 1638 cm^{-1} are visible. The peak at 686 cm^{-1} was due to the stretching vibration of Si-O-C and strong interaction of Si-O are noticeable at 1100 cm^{-1} and 1053 cm^{-1} (Figure 2B) This results confirms that the amine group was modified by the surface epoxy, hydroxyl and carboxyl groups of graphene materials. In the Figure 2B (c), the peak at 564 cm^{-1} was due to Pd-N stretching frequencies [36] confirming that Pd nanoparticles were bound to the amine group.

The quality and quantity of graphene layers can be investigated using Raman spectroscopy. The Raman spectra of GO, AAPTMS@GO and Pd(0)-AAPTMS@G are shown in Figure 3. In these spectra, the entire sample exhibited the characteristic D, G and 2D bands at 1342 , 1560 and 2675 cm^{-1} . The conformation of disorder in the sp^2 -hybridized carbon atoms in graphene sheets is from D-band of Raman spectra, while G band corresponds to σ - sp^2 bonded C-atoms. In our materials, D band was very small, indicating negligible disorder in the structure of material. The 2D band gives the information about number of layers is presented in materials [37-39]. The absence of D-band as well as shapes of 2D-band suggest that after generation of Pd nanoparticle, the amine functionalized graphene oxide possibly gets converted to single layer amine functionalized graphene [40].

The SEM images of GO, diamine functionalized graphene oxide, Pd nanoparticle supported on amine functionalized graphene and higher magnification of nanoparticles are shown in Figure 4. The amine functionalized graphene consist of randomly aggregated thin sheets forming a disordered network and also surface roughness increases compared with GO, due to

successful exfoliation (Figure 4a & 4b). The spherical Pd nanoparticles were bounded to the amine group, which obtained in each layer and also on the edges of the graphene sheet are shown in Figure 4c & 4d).

Energy-dispersive X-ray spectroscopy gives the information on the type of element present in the particular area. The EDX image of GO and Pd(0)-AAPTMS@G is shown in Figure 5. From the spectra, it can be seen that only carbon is present in the GO materials (Figure. 5a), while silicon, carbon, nitrogen, and Pd are present in the Pd(0)-AAPTMS@G sample (Figure. 5b). The SEM-EDX is correlated with the ICP analysis.

TEM image of (a) GO, (b) AAPTMS@GO, (c) Pd (0)-AAPTMS@G, and (d) Higher magnification of Pd (0)-AAPTMS@G are shown in Figure 6. The successful exfoliation of graphite oxide converted to single-layer sheet in Figure 6(a). The net-like structure was appeared after modification of the organic group over the GO surface (Figure. 6b). The black spots appearing in Figure 6c represent the existence of nanoparticles. The uniform distribution of nanoparticles on the organic surface is also observable.

The uniform distribution of Pd nanoparticles on the of amine group bonded to the surface functional group on the single layer graphene is shown in Figure 7a & 7c. The Pd nanoparticle was stable relative to the basic organic group and facilitates the product formation. The size of Pd nanoparticles was 3 nm to 7 nm and the average particle size was 5.5 nm (Figure. 7b & 7d). The size of the nanoparticles can influence the productivity in the coupling reactions. Harada et al. [41] reported that relatively more active sites exist on the smaller Pd nanoparticles, leading to better catalytic activity. The TEM of reused catalyst is illustrated in Figure 7e. No obvious alteration in morphology was observed for Pd nanoparticles after coupling reactions in used catalyst. The binding energy of Pd $3d^{5/2}$ and Pd $3d^{3/2}$ corresponds to 335.55 and 340.94 eV is shown in (Figure 7f), which is similar to Pd (0). Hence it can be proposed that the

developed particles were nano sized, highly stable, and reusable for better productivity of coupling products.

Many researchers have reported the C-C coupling reactions in organic solvents and inert conditions using different catalysts on acidic support. However, there are very few examples with Pd as catalyst. The C-C coupling reaction over palladium modified montmorillonite catalyst, at high temperature (150 °C) with reaction time (2-3 h) and 92% yield was reported [42]. Corral et al., have reported 35 % conversion towards C-C coupling reaction within 3 h in presence of organic solvent [43]. The inherent disadvantages in these reports were need for organic solvent, high temperature and longer reaction times. Literature shows that in Suzuki coupling reaction, many different bases like Na₂CO₃, Cs₂CO₃, K₂CO₃, KF and NaOH were used in stoichiometric proportions [44]. In the current study Ba(OH)₂ or K₃PO₄ were successfully employed as a base, with no need to use stoichiometric amounts.

In this communication, we report the use of AAPTMS@GO with basic support. The catalytic activity of Pd substituted amine functionalized graphene hybrids in the formation of biaryl C–C bonds was examined for the Suzuki coupling reaction of halobenzene with phenylboronic acid in the aqueous medium (Scheme 1) which gave excellent yield (98%) with short reaction time (< 30 min). To compare the activity of these materials, the reaction was carried out with GO, AAPTMS@GO Pd(0)-AAPTMS@G and Pd/rGO as catalysts under otherwise identical conditions (Table. 1). Results indicate that the C-C coupling reaction through the reductive elimination process over Pd(0)-AAPTMS@G gave excellent yield, while others showed poor performance. Oxidative addition of phenyl halides in the presence of catalyst is the key step in the proposed mechanism (Scheme 2).

A perusal of results in Table 1 clearly show that Ba(OH)₂ or K₃PO₄ as base have facilitated good yield of cross-coupling reaction product.

We examined the further scope of the method using other halo benzenes and halo pyridines

as starting materials (Table. 2). The bond energies of C–Cl, C–Br and C–I bonds are 340.2, 281.4 and 222.6 kJmol⁻¹ respectively. The C–I bond easily breaks and to form C–C product as compared to other. The Pd (0)-AAPtMS@G catalyst gave relatively lower yields for Cl-substituents, but was efficient for reactions between Br-substituted pyridines or Br-substituted benzenes in the C–C coupling giving good yields. Turner et al. have reported that the small sized Pd nanoparticles give the better catalytic properties [45]. The ability to control the size of the Pd nanoparticles with basic support onto the amine functionalized graphene is therefore an advantage of our method. With the aid of basic support, the stability and activity of Pd nanoparticles on graphene was impressive, possibly due to adequate electron density on attached Pd (0) species, which accelerated the oxidative addition of halobenzene to Pd (0).

To optimise the catalyst loading, its effect on the yield % of biphenyl was studied over Pd(0)AAPtMS@G was investigated (Figure 8). The yield% increased from 87% to 98% with increase in the catalyst amount from 0.02 to 0.05 g, but no enhanced yield was recorded with higher amount of catalyst. 0.06 g gave 98% yield only.

In heterogeneous catalysis, the reusability of the catalyst is paramount and it primarily depends on the stability and the ease of separation of the catalyst. The activity of catalyst can change due to the coke formation on the catalyst surface and due to leaching of some nanoparticles into the reaction medium. Hence to test its robustness, the recovered catalyst was reused after regeneration by calcination in the reaction for six consecutive cycles. No noticeable change was observed with activity remaining intact (Table 3). The catalyst did not leach out in aqueous medium because of the strong interaction between organo amino group and nanoparticles. The 7th cycle to onwards some reduction in its efficiency was noticed from ICP analysis. The ICP analysis demonstrates that after five repetitive uses of the catalyst in the coupling reactions, the decrease in Pd concentration was < 0.8% relative to original sample,

suggesting that leaching was negligible, but after the seventh and eighth runs, the leached amount of Pd was ~10% and ~15 % respectively.

Turnover frequency (TOF) a measure of efficiency of catalyst totally depends on the Pd concentration, which reflects the structural development of supported palladium. Mulhaupt et al., reported that Suzuki coupling reaction over Pd²⁺ exchanged graphite oxide catalyst gives turnover frequency [TOF = 39000 h⁻¹ (650 min⁻¹)] [46]. Siamaki et al., have observed that coupling reaction over Pd/G catalyst gave [TOF = 108,000 h⁻¹ (1800 min⁻¹)] [47]. Nie et al., reported that Suzuki coupling reaction over Pd–Ni/RGO catalyst gave [TOF = 38,750 h⁻¹ (645.83 min⁻¹)] [48]. In the current study using Pd(0)-AAPTMS@G as catalyst, higher TOF [185,078 h⁻¹ (3084.64 min⁻¹)] and excellent conversion (100%) up to 6th run were observed for the C-C Suzuki coupling reaction.

A comparison of various parameters for C-C Suzuki coupling reaction with various reported catalysts is summarized in Table 3. An examination of the data in table 3 shows that proposed method proves superior with better TOF, excellent conversions, longer reusability and no need for solvent, relative to earlier reported catalysts which need organic solvent/ higher reaction times and short catalyst lives. Through some systems also got excellent results, the use of organic solvent is not so environmentally benign. Wang et al. have reported the reaction using ethanol as an organic solvent, with the help of Pd/graphene catalyst and got 100% conversion [54]. Therefore the effectiveness of our new catalyst in absence of any organic solvent and high TOF is rewarding.

FT-IR spectra for regenerated catalysts are shown in Figure 9. It can be seen that though there is a decrease in intensity, the spectra of the reused catalysts are quite similar to that of the fresh one in figure 2. This confirms the retention of catalyst structure. All these experimental evidences suggest the catalyst to be truly heterogeneous.

4. Conclusions:

In conclusion, the Pd nanoparticles supported on amine functionalized graphene were successfully prepared by a simple procedure and the catalyst was found to be efficient (98 % yield), highly stable, reusable and excellent TOF (3084.64 min^{-1}) for C-C coupling reactions. The Raman study revealed that the catalyst was single layer graphene. As confirmed by the FTIR and TEM analysis, organic group was covalently bound onto graphene layer. TEM confirmed that Pd nanoparticles (3 - 7 nm) were uniformly distributed over the surface of amine functionalized graphene. The recovered catalyst can be reused after regeneration by calcination.

Acknowledgement

The authors acknowledge the support received from the School of Chemistry & Physics and College of Agriculture, Engineering & Science, University of KwaZulu-Natal, Durban, South Africa in the form of research facilities and financial support.

References

- [1] L.V. Radushkevich, M.V. Lukyanovich, J. Phys. Chem. 26 (1952) 88-95.
- [2] S. Iijima, Nature 1991, 354, 56-58.
- [3] R. H. Baughman, A. A. Zakhidov, W. A. De Heer, Science 297(2002) 787-792.
- [4] J. Kong, N.R. Franklin, C. Zhou, M.G. Chapline, S. Peng, K. Cho, H. Dai, Science 287(2000) 622-625.
- [5] G. Chen, T.M. Paronyan, E.M. Pigos, A.R. Harutyunyan, Sci. Rep. 2 (2012) 1.
- [6] M. Castro, J. Lu, S. Bruzard, B. Kumar, J. F. Feller, Carbon 47 (2009) 1930-1942.
- [7] B. Kumar, M. Castro, J. F. Feller, J. Mater. Chem. 22 (2012) 10656–10664.
- [8] H. C. Nerl, C. Cheng, A. E. Goode, S. D. Bergin, B. Lich, M. Gass, A. E. Porter, Nano medicine 6 (2011) 849–865.

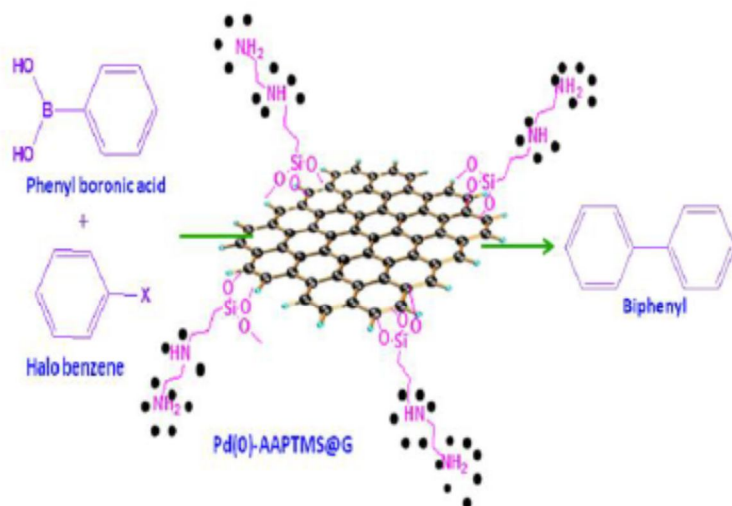
- [9] M. J. Allen, V. C. Tung, R. B. Kaner, *Chem. Rev.* 110 (2010) 132 – 145.
- [10] A. K. Geim, K. S. Novoselov, *Nat. Mater.* 6 (2007) 183–191.
- [11] D. Yu, L. Dai, *J. Phys. Chem. Lett.* 1 (2010) 467 – 470.
- [12] Y. Liu, D. Yu, C. Zeng, Z. C. Miao, L. Dai, *Langmuir* 26 (2010) 6158 – 6160.
- [13] A. K. Geim, *Science* 324 (2009) 1530–1534.
- [14] R. R. Nair, P. Blake, A. N. Grigorenko, K. S. Novoselov, T. J. Booth, T. Stauber, N. M. R. Peres, A. K. Geim, *Science* 320 (2008) 1308–1308.
- [15] Y. Zhu, S. Murali, W. Cai, X. Li, J. W. Suk, J. R. Potts, R. S. Ruoff, *Adv. Mater.* 22 (2010) 3906–3924.
- [16] S. Park, R. S. Ruoff, *Nat. Nanotechnol.* 4 (2009) 217–224.
- [17] L. T. Qu, Y. Liu, J. B. Baek, L. Dai, *ACS Nano* 4 (2010) 1321 – 1326.
- [18] D. R. Dreyer, S. Park, C. W. Bielawski, R. S. Ruoff, *Chem. Soc. Rev.* 39(2010) 228–240.
- [19] X. Huang, Z. Yin, S. Wu, X. Qi, Q. He, Q. Zhang, Q. Yan, F. Boey, H. Zhang, *Small* 7 (2011) 1876–1902.
- [20] X. Li, W. Cai, J. An, S. Kim, J. Nah, D. Yang, R. Piner, A. Velamakanni, I. Jung, E. Tutuc, *Science* 324 (2009) 1312–1314.
- [21] N. Li, Z. Y. Wang, K. K. Zhao, Z. J. Shi, Z. N. Gu, S. K. Xu, *Carbon* 48 (2010) 255–259.
- [22] A. Hashimoto, K. Suenaga, K. Urita, T. Shimada, T. Sugai, S. Bandow, H. Shinohara, S. Iijima, *Phys. Rev. Lett.* 94 (2005) 045504–045520.
- [23] W. S. Hummers, R. E. Offeman, *J. Am. Chem. Soc.* 80 (1958) 1339–1339.
- [24] C.Y. Su, Y. Xu, W. Zhang, J. Zhao, A. Liu, X. Tang, C.H. Tsai, Y. Huang, L.J. Li, *ACS Nano* 4 (2010) 5285–5292.

- [25] L. Stobinski, B. Lesiaka, A. Malolepszy, M. Mazurkiewicz, B. Mierzwa, J. Zemek, P. Jiricek, I. Bieloshapka, *J. Elect. Spect. Rel. Phen.* 195 (2014) 145–154.
- [26] P. Gnanaprakasam, T. Selvaraju, *RSC Adv.* 4 (2014) 24518–24525.
- [27] P. Sharma, A. P. Singh, *Catal. Sci. Technol.* 4 (2014) 2978-2989.
- [28] S. Rana, S. Maddila, S.B. Jonnalagadda, *Catal. Sci. Technol.*, 2015, DOI: 10.1039/C5CY00192G.
- [29] G. B. B. Varadwaj, S. Rana, K. M. Parida, *J. Phys. Chem. C* 118 (2014) 1640–1651
- [30] G. Lu, S. Mao, S. Park, R.S. Ruoff, J. Chen, *Nano Res.* 2 (2009) 192–200.
- [31] Y. J. Li, W. Gao, L. J. Ci, C. M. Wang, P. M. Ajayan, *Carbon* 48 (2010) 1124-1126.
- [32] H. K. Jeong, Y. P. Lee, R. J. W. E. Lahaye, M. H. Park, K. H. An, I. J. Kim, C.-W. Yang, C. Y. Park, R. S. Ruoff, Y. H. Lee, *J. Am. Chem. Soc.* 130 (2008) 1362-1366.
- [33] J. J. Niu, J. N. Wang, *Electrochim. Acta* 53 (2008) 8058-8063.
- [34] R. N. Singh, R. Awasthi, *Catal. Sci. Technol.* 1 (2011) 778–783.
- [35] P. F. Li, H. Zhou, X. Cheng, *Surface & Coatings Techno.* 254 (2014) 298–304.
- [36] K. Mukhopadhyay, B. R. Sarkar, and R. V. Chaudhari, *J. Am. Chem. Soc.* 124 (2002) 9692-9693.
- [37] C. Casiraghi, S. Pisana, K. S. Novoselov, A. K. Geim, A. C. Ferrari, *Appl. Phys. Lett.* 91 (2007) 23108-23114.
- [38] A. C. Ferrari, J. C. Meyer, V. Scardaci, C. Casiraghi, M. Lazzeri, F. Mauri, S. Piscanec, D. Jiang, K. S. Novoselov, S. Roth, *Phys. Rev. Lett.* 97 (2006) 187401-187415.
- [39] N. R. Wilson, P.A. Pandey, R. Beanland, R. J. Young, I. A. Kinloch, L. Gong, Z. Liu, K. Suenaga, J. P. Rourke, S. J. York, J. Sloan, *ACS Nano* 3 (2009) 2547–2556.

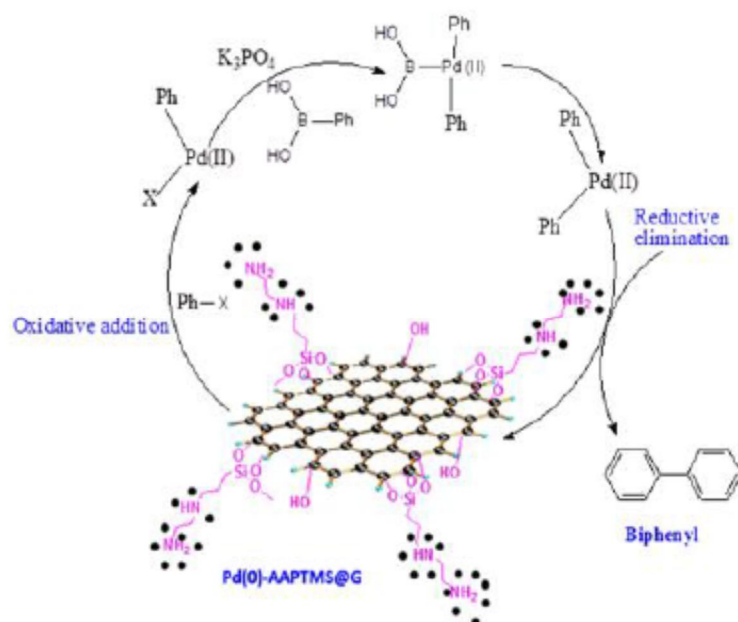
- [40] A. Esaú Del Rio-Castillo, C. Merino, E. Díez-Barra, E. Vázquez, *Nano Res.* 7(7) 2014, 963–972.
- [41] T. Harada, S. Ikeda, M. Miyazaki, T. Sakata, H. Mori, M. Matsumura, *J. Mol. Catal. A-Chem.* 268 (2007) 59–64.
- [41] Árpád Molnár, Attila Papp, *Synlett* 18 (2006) 3130-3134.
- [42] J. A. Corral, M. I. López, D. Esquivel, M. Mora, S. Jiménez-Sanchidrián, F.J. Romero-Salguero, *Materials* 6 (2013) 1554-1565.
- [43] S. Kotha, K. Lahiri, and D. Kashinath, *Tetrahedron* 58 (2002) 9633-9695.
- [44] M. Turner, V. B. Golovko, O. P. H. Vaughan, P. Abdulkin, A. Berenguer-Murcia, M. S. Tikhov, B. F. G. Johnson, R. M. Lambert, *Nature* 454 (2008) 981–983.
- [45] Gil M. Scheuermann, L. Rumi, P. Steurer, W. Bannwarth, and R. Mulhaupt, *J. Am. Chem. Soc.* 131 (2009) 8262–8270.
- [46] A.R. Siamaki, Abd El. Rahman S. Khder, V. Abdelsayed, M. S. El-Shall, B. F. Gupton, *Journal of Catalysis* 279 (2011) 1–11.
- [47] R. Nie, J. Shi, W. Du, Z. Hou, *Applied Catalysis A: Gen.* 473 (2014) 1–6.
- [48] Y. Li, X. Fan, J. Qi, J. Ji, S. Wang, G. Zhang, and F. Zhang, *Nano Res.* 3 (2010) 429–437.
- [49] Shun-ichi. Yamamoto, H. Kinoshita, H. Hashimoto, and Y. Nishina, *Nanoscale* 6 (2014) 6501–6505.
- [50] S. Moussa, A. R. Siamaki, B. F. Gupton, and M. Samy El-Shall, *ACS Catal.* 2 (2012) 145–154.
- [51] S. Santra, P. K. Hota, R. Bhattacharyya, P. Bera, P. Ghosh, and S.K. Mandal, *ACS Catal.* 3 (2013) 2776–2789.
- [52] L. Rumi, G. M. Scheuermann, R. Mulhaupt, and W. Bannwarth, *Helv. Chim. Acta.* 94 (2011) 966-973.

[53] G. Xiang, J. He, T. Li, J. Zhuang, and X. Wang, *Nanoscale* 3 (2011) 3737–3742.

Scheme 1 Schematic diagram of C-C coupling reaction over Pd(0)-AAPTMS@G catalyst



Scheme 2 Mechanism of C-C coupling reaction over Pd(0)-AAPTMS@G catalyst



List of Figures

Figure 1 XRD spectra of GO (a) and Pd(0)-AAPTMS@G.

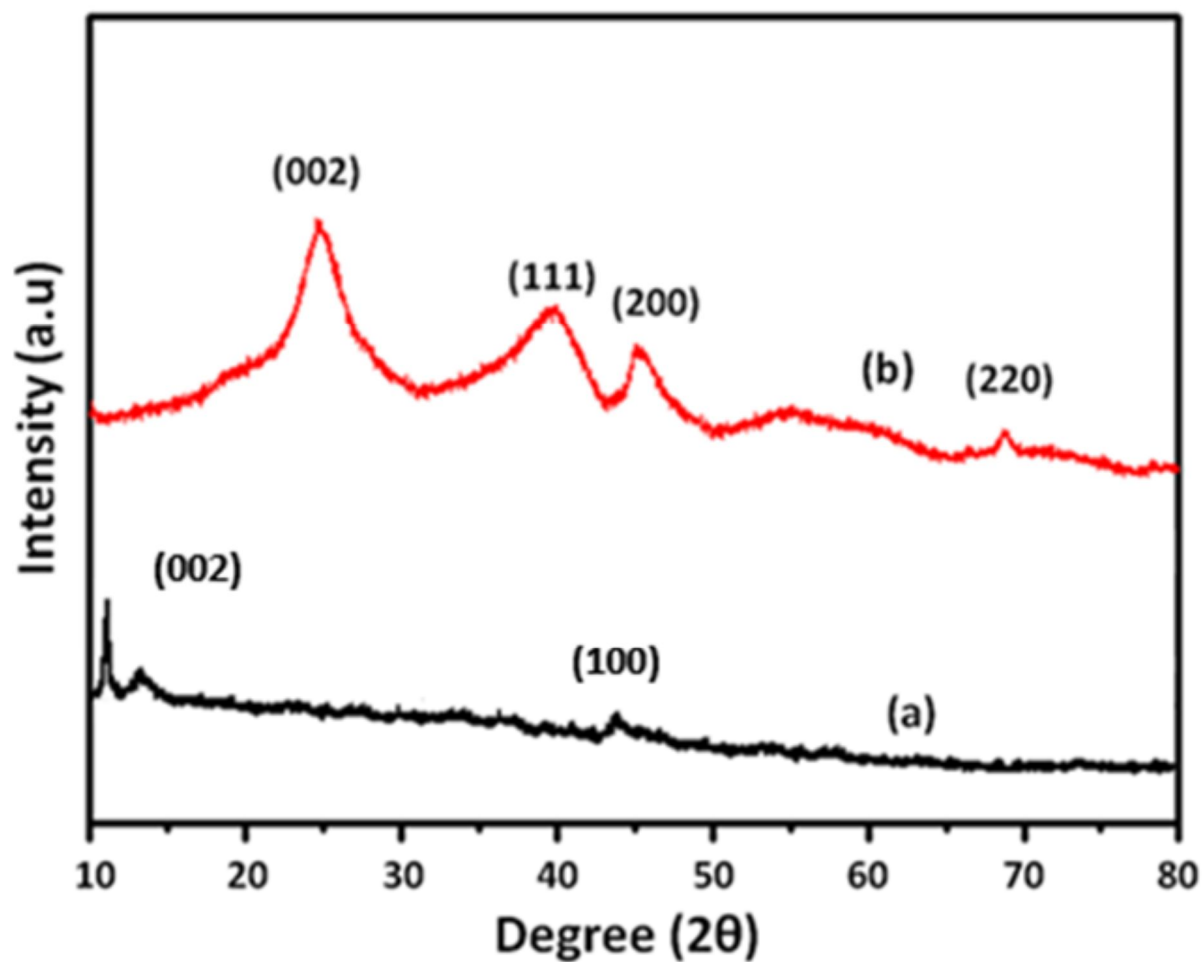


Figure 2A FT-IR spectra (4000-400) of GO (a), AAPTMS@GO (b) and Pd(0)-AAPTMS@G (c) samples.

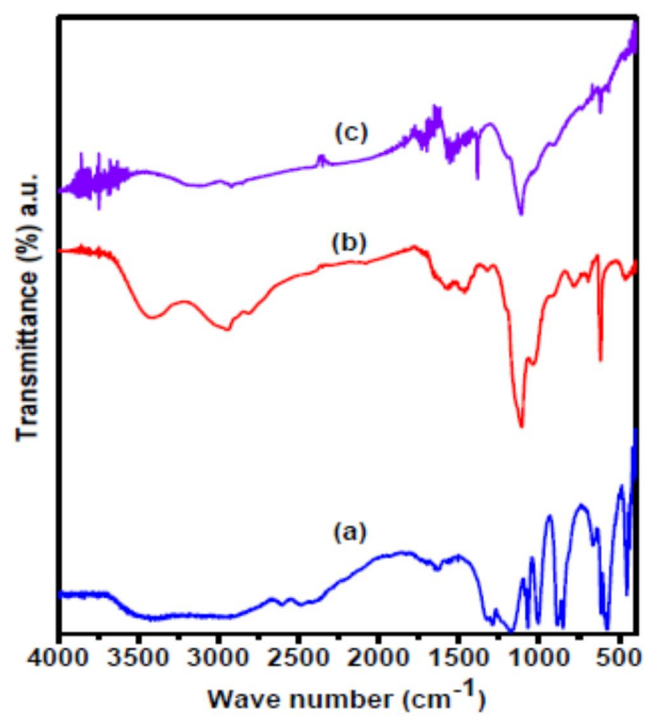


Figure 2A

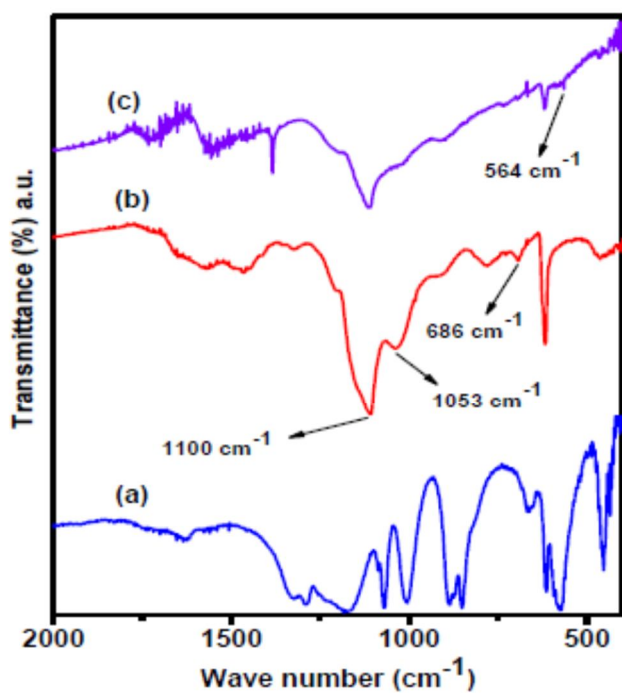


Figure 2B

Figure 2B FT-IR spectra (2000-400) of GO (a), AAPTMS@GO (b) and Pd(0)-AAPTMS@G (c) samples.

Figure 3 Raman spectra of GO (a), AAPTMS@GO (b) and Pd(0)-AAPTMS@G (c) materials.

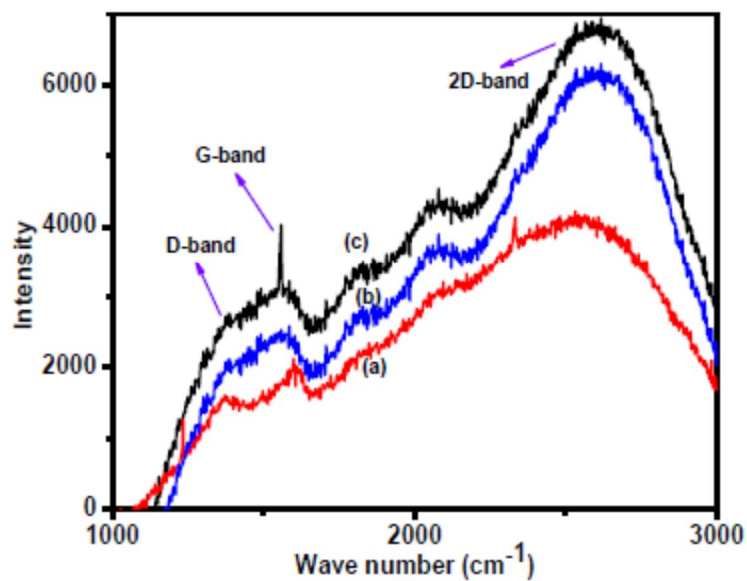


Figure 4 SEM Image of (a) GO, Scale bar = 200 nm (b) AAPTMS@GO, Scale bar = 100 nm, (c) Pd(0)-AAPTMS@G, Scale bar = 2 μm and (d) Higher magnification of Pd(0)-AAPTMS@G, Scale bar = 200 nm.

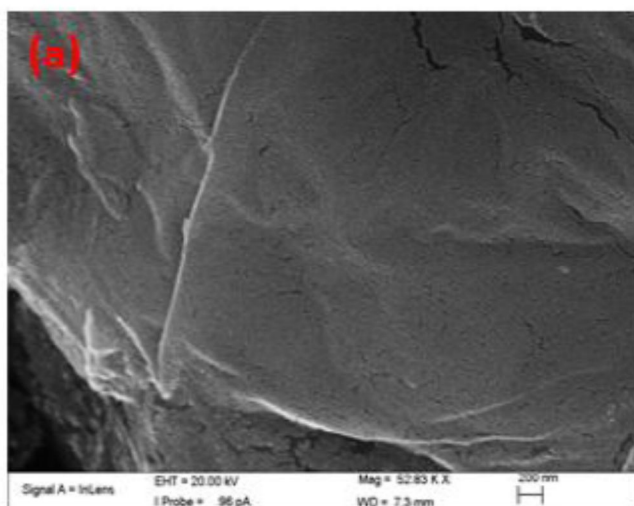


Figure 4 (a)

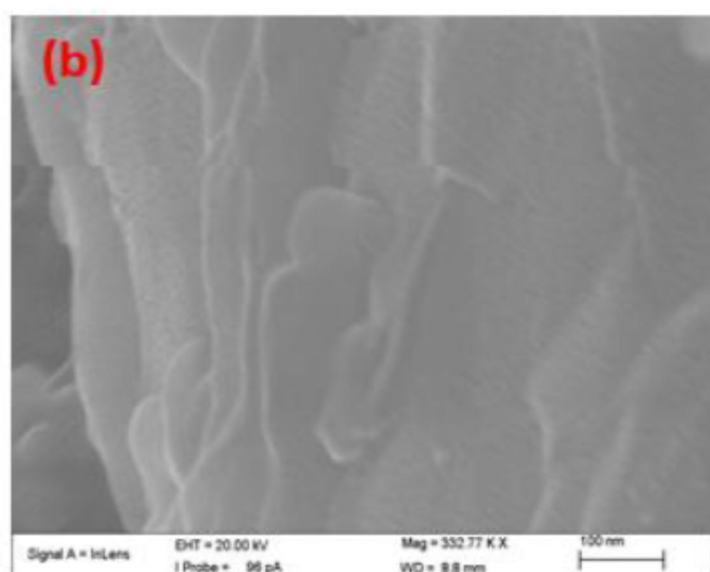


Figure 4 (b)

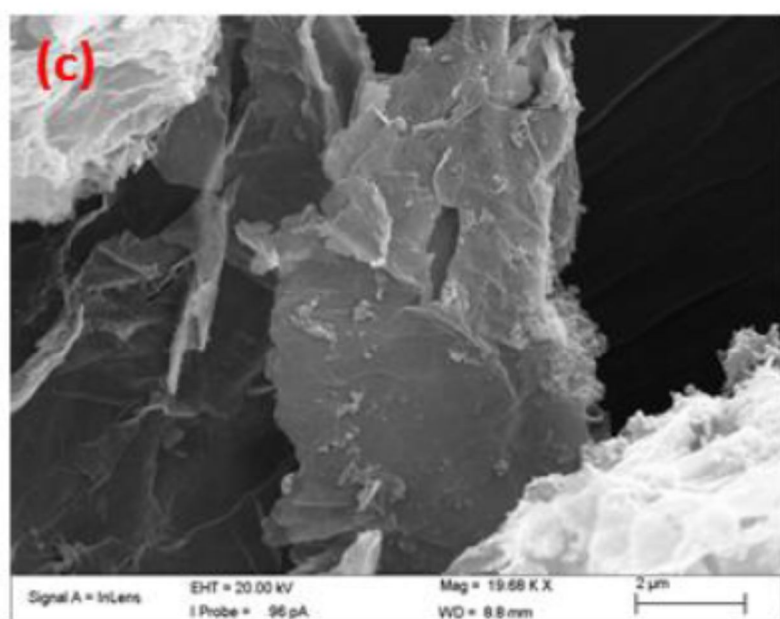


Figure 4 (c)

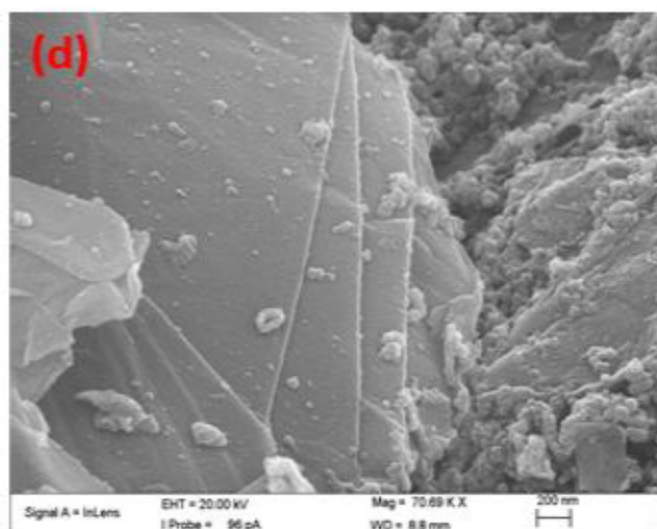


Figure 4(d)

Figure 5 EDX Image of (a) GO, and (b) Pd(0)-AAPtMS@G sample.

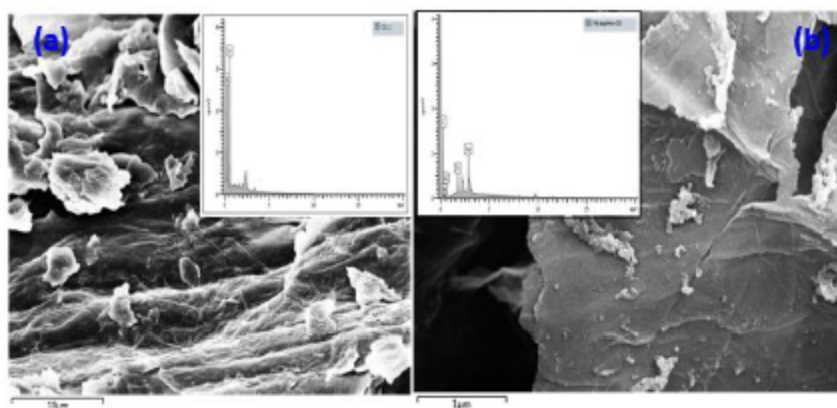


Figure 5

Figure 6 TEM Image of (a) GO, scale bar =100 nm (b) AAPtMS@GO, scale bar =100 nm (c) Pd (0)-AAPtMS@G, scale bar =100 nm and (d) Higher magnification of Pd (0)-AAPtMS@G, scale bar = 50 nm.

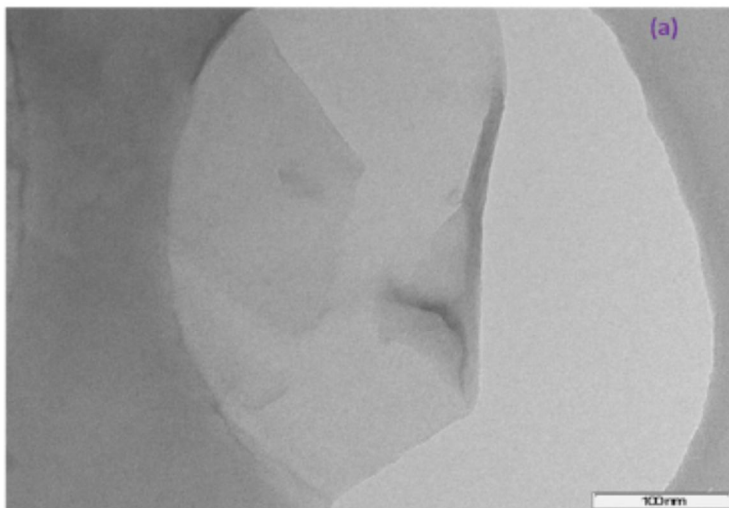


Figure 6 (a)

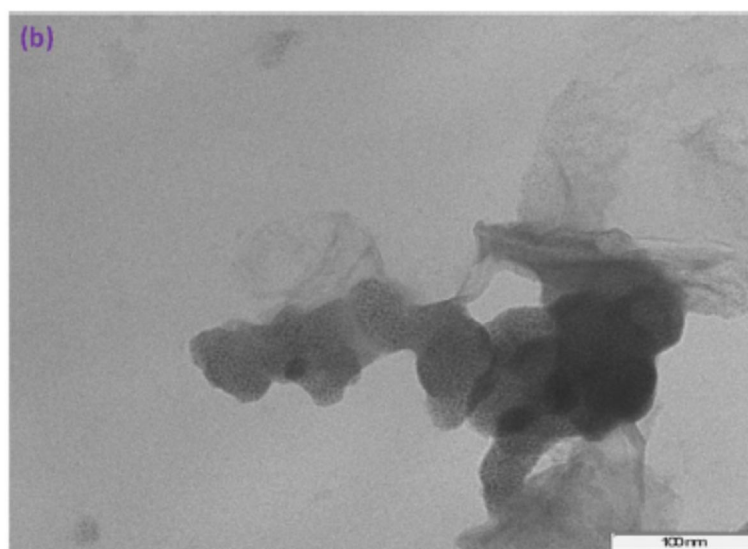


Figure 6 (b)

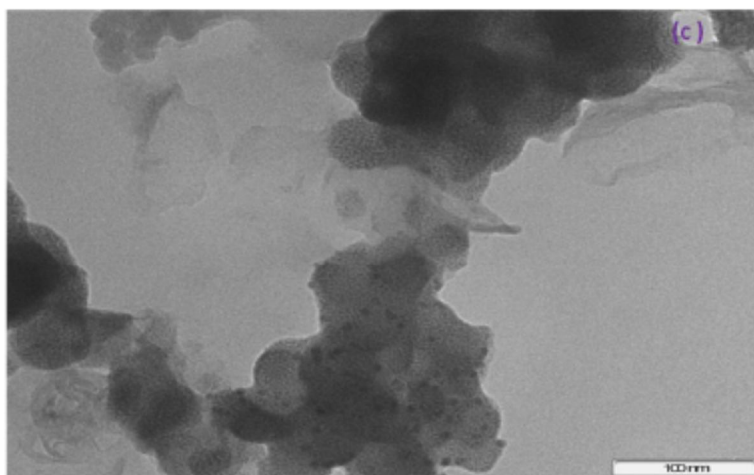


Figure 6 (c)

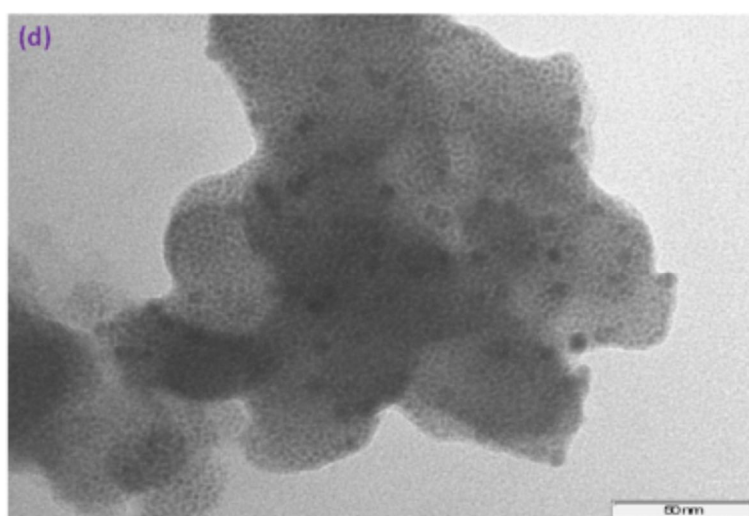


Figure 6 (d)

Figure 7 TEM image of (a) Pd nanoparticles, Scale bar = 50 nm (b) Histogram of the particle size distribution for the Pd nanoparticles, (c) Pd nanoparticles, Scale bar =100 nm (d) Histogram of Pd nanoparticles, (e) TEM image of the recycled catalyst, Scale bar = 50 nm and (f) XPS spectra of Pd nanoparticle.

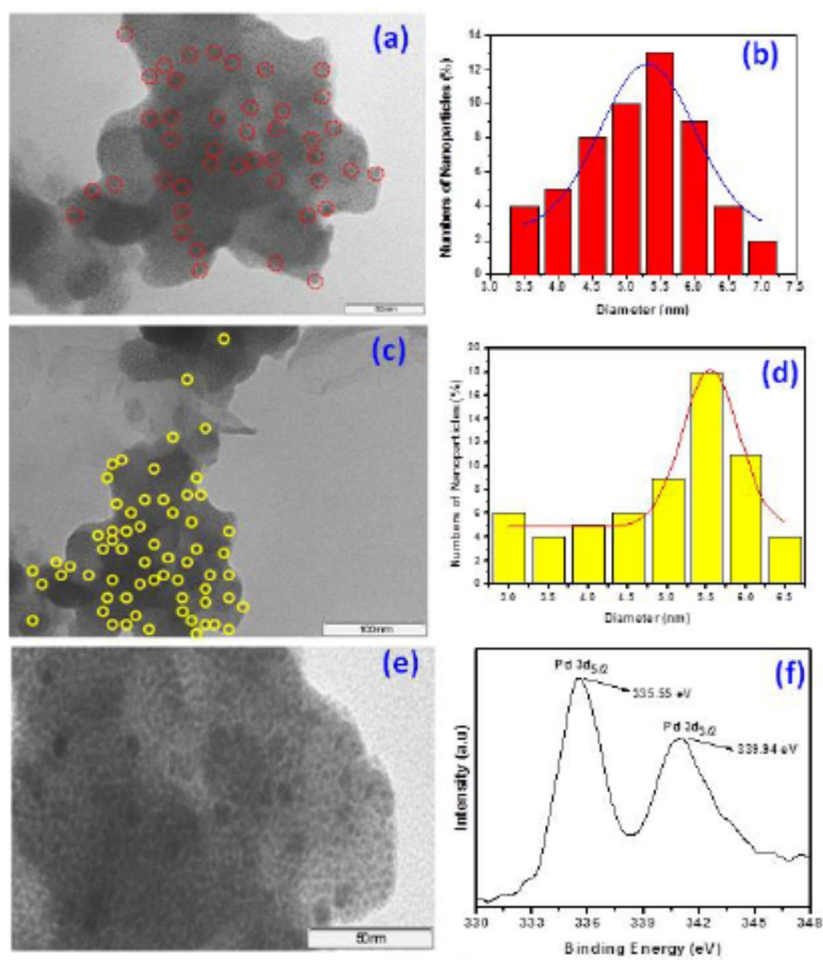


Figure 7

Figure 8 Influence of the catalyst amount on C-C coupling reaction of biphenyl at constant time, temperature and solvent.

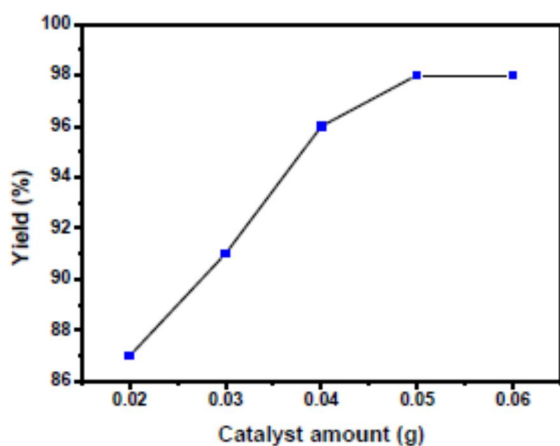


Figure 8

Figure 9 FTIR spectra of reused catalyst.

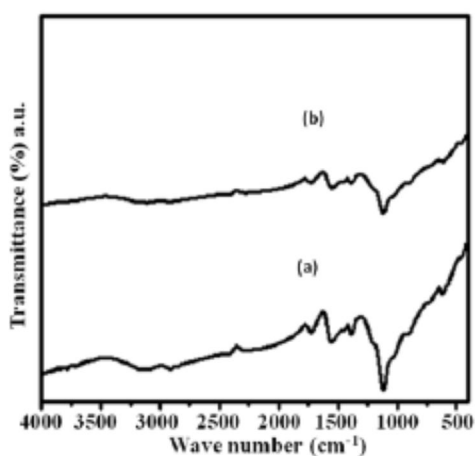


Figure 9

List of Tables

Table-1 Activity of Various Catalysts toward C-C coupling reaction ^[a].

Catalyst	Yield (%)	[a]	Reaction conditions:
GO	-----		temperature, 90 °C;
AAPTMS@GO	11		time, 25 minute;
			catalyst, 0.05 g;
			solvent (water), 20

Pd(II)AAPTMS@GO	74	mL.	Reactants:	
Pd(0)AAPTMS@G	98	iodobenzene	(1	
Pd/rGO	96	phenylboronic acid	mmol);	
<hr/>			(1.2	mmol);
phosphate (0.0018 mmol).			tripotassium	

Table 2: Effect of different substrate on C-C coupling reaction^[a] over Pd (0)-AAPPTMS@G catalyst.

Entry	Substrate	Yield (%)	Products
1		98	
2		79	
3		33	
4		96	
5		84	
6		32	
7		43	

^[a]Reaction conditions: temperature, 90 °C; time, 25 minute; catalyst, 0.05 g; solvent (water), 20 ml. Reactants: iodobenzene (1mmol); phenylboronic acid (1.2 mmol); tripotassium phosphate (0.0018 mmol).

Table 3: Comparison study of C-C coupling reaction catalyzed by Pd(0) in a variety supported catalysts

Catalyst	Solvent	Temp. (°C)	Time (min)	Conv. (%)	Yield (%)	No. of recycle with yield (%) ^a /conversion (%) ^b									Reference
						1 st	2 nd	3 rd	4 th	5 th	6 th	7 th	8 th	9 th	
Pd(0)-AAPTMS@G	Water	90	25	100	98	98 ^a	98 ^a	98 ^a	97 ^a	98 ^a	97 ^a	88 ^a	82 ^a	84 ^a	Present work
Pd ²⁺ -GO	Ethanol & Water	80	240	100	100	100 ^a	83 ^a	74 ^a	19 ^a	-	-	-	-	-	[46]
Pd-Ni/RGO	Ethanol & Water	30	300	-	98.6	-	-	-	-	-	-	-	-	-	[48]
Pd-graphene	Water	100	5	-	100	100 ^a	93.5 ^a	84.7 ^a	87.1 ^a	88.3 ^a	92.7 ^a	84.6 ^a	93.0 ^a	79.7 ^a	[49]
Pd-slGO	Ethanol	RT	60	-	44	-	-	-	-	-	-	-	-	-	[50]
Pd/PRGO	Ethanol & Water	80	5	100	-	100	100 ^b	86 ^b	63 ^b	50 ^b	38 ^b	24 ^b	-	-	[51]
GO-PdNPs	Toluene	110	1440	-	85	-	-	-	-	-	-	-	-	-	[52]
GO-PdNPs	Water	100	740	-	61	-	-	-	-	-	-	-	-	-	[52]
Pd ²⁺ /GO	DMA/H ₂ O	80	1440	90	85.5	-	-	-	-	-	-	-	-	-	[53]